Distinct mechanisms of CB1 and $GABA_B$ receptor presynaptic modulation of striatal indirect pathway projections to mouse Globus Pallidus

Giacomo Sitzia[1,2], Karina Possa Abrahao[3], Daniel Liput[1], Gian Marco Calandra[4], David M. Lovinger*[1]

[1] Current address: Laboratory for Integrative Neuroscience, National Institute on Alcohol Abuse and Alcoholism, US National Institutes of Health, Rockville, USA

[2] Molecular Neurophysiology Laboratory, Department of Physiology and Pharmacology, Karolinska Institutet, Stockholm, Sweden

[3] Departamento de Psicobiologia, Universidade Federal de São Paulo, Campus São Paulo, São Paulo, SP, Brazil

[4]Institute for Stroke and Dementia Research, Ludwig-Maximilians-Universität, Munich, Germany.

Email: Giacomo.sitzia@ki.se, lovindav@mail.nih.gov

Corresponding Author information: *David M. Lovinger (lovindav@mail.nih.gov).

Laboratory for Integrative Neuroscience, National Institute on Alcohol Abuse and Alcoholism, National Institutes of Health, Maryland, 20852, USA, Orcid: 0000-0002-5454-6725

Abstract

Presynaptic modulation is a fundamental process regulating synaptic transmission. Striatal indirect pathway projections originate from A2A- expressing spiny projection neurons (iSPNs), targeting the globus pallidus external segment (GPe) and control the firing of the tonically active GPe neurons via GABA release. It is unclear if and how the presynaptic GPCRs, $GABA_B$ and CB1 receptors, modulate iSPN projections. Here we used an optogenetic platform to study presynaptic Ca^{2+} and GABAergic transmission at iSPN projections, using a genetic strategy to express the calcium sensor GCaMP6f or the excitatory channelrhodopsin (hChR2) on iSPNs. We found that P/Q-type calcium channels are the primary VGCC-subtype controlling presynaptic calcium and GABA release at iSPN-GPe projections. N-type and L-type VGCCs contribute to GABA release at iSPN-GPe projections. $GABA_B$ receptor activation resulted in a reversible inhibition of presynaptic Ca^{2+} transients (PreCaTs) and an inhibition of GABAergic transmission at iSPN-GPe synapses. CB1 receptor activation did not inhibit PreCaTs while inhibiting GABAergic oIPSCs at iSPN-GPe synapses. CB1 effects on GABAergic transmission persisted in experiments where Na_V and K_V1 were blocked, indicating a VGCC- and K_V1 independent presynaptic mechanism of action of CB1 receptors. Taken together, presynaptic modulation of iSPN-GPe projections by CB1 and $GABA_B$ receptors is mediated by distinct mechanisms.

Introduction

The dorsal striatum (DS) is the main input structure of the basal ganglia (BG), a group of subcortical regions involved in motor control, associative learning and decision making. Spiny projection neurons (SPNs) constitute up to 95% of neurons in the rodent striatum (Graveland & Di Figlia, 1985) and are classified based on their molecular markers and projection targets, into direct pathway spiny projecting neurons (dSPNs) and indirect pathway SPNs (iSPNs) (Gerfen et al., 1990). The dSPNs express the dopamine D1 receptor and project to the substantia nigra pars reticulata (SNr), the entopeduncular nucleus (EPN) and, through axonal collaterals, to the globus pallidus external segment (GPe) (Chang et al., 1981). iSPNs express dopamine D2 and adenosine A2A receptors and project to the GPe. Neurons in the GPe are tonically active, and this activity is influenced by GABAergic inputs from the iSPNs. Presynaptic neuromodulation by GPCRs controls GABA release in the GPe (Engler et al., 2006) but the synapse- specific mechanisms are unclear. Thus, understanding how GPCRs govern presynaptic calcium entry and neurotransmitter release at the iSPN projections in the GPe is fundamental in determining how the striatum exerts control over its downstream targets, in physiology and in disease.

Two key modulators of GABAergic transmission in the GPe are the $G_{i/o}$ coupled cannabinoid type 1 (CB1) and $GABA_B$ receptors, and these receptors are thought to act predominantly through presynaptic inhibition of GABA release (Engler et al., 2006; Kaneda & Kita, 2005). Expression levels of CB1 receptors on striatal terminals in the GPe and SNr are among the highest in the CNS (Davis et al., 2018; Hu & Mackie K., 2015). CB1 receptors expressed in SPNs control exploratory behaviors and motor coordination (Bonm et al., 2021). Activation of CB1 receptors controls striatal output by reducing neurotransmitter release at striatonigral (Wallmichrath & Szabo, 2002; Borgqvist et al., 2015) and striatopallidal (Engler et al., 2006) synapses. Furthermore, $GABA_B$ receptors are expressed at striatonigral (Boyes & Bolam 2003) and striatopallidal synapses (Chen et al, 2004). $GABA_B$ receptors control striatal output by reducing GABA release at GABAergic synapses in the GPe (Kaneda & Kita, 2005). As slice preparations where neurotransmitter release is evoked through electrical stimulation fail to distinguish the activation of specific striatal output pathways, it remains unclear if and how CB1 and $GABA_B$ receptors modulate transmission specifically at iSPN-GPe projections.

CB1 and $GABA_B$ receptors suppress neurotransmitter release in the CNS through downstream signaling cascades mediated by the $G_{\beta\gamma}$ subunit, including inhibition of voltage-gated calcium channels (VGCCs), inhibition of the vesicle release complex downstream of Ca^{2+} entry, and activation of K^+ channels (Araque et al., 2017; Chalifoux & Carter, 2011). Mechanisms involving the Gαi/Go subunits, including the inhibition of cAMP/ PKA signaling, also influence neurotransmitter release (Araque et al., 2017; Chalifoux & Carter, 2011). The downstream mechanisms engaged by CB1 and $GABA_B$ receptors are synapse specific and can be non- canonic. In the nucleus accumbens, CB1 receptors suppress neurotransmitter release at cortico-accumbal synapses through a VGCC-independent, K^+ channel-dependent mechanism (Robbe et al., 2001), while $GABA_B$ receptors inhibit neurotransmitter release at glutamatergic synapses through a VGCC-independent, SNAP25-dependent mechanism (Manz et al., 2019). In the dorsal striatum, $GABA_B$ receptors suppress neurotransmitter release at corticostriatal synapses through inhibition of presynaptic VGCCs (Kupfershmidt & Lovinger, 2015).

Here we studied the mechanisms mediating presynaptic Ca^{2+} entry and GABAergic transmission on the indirect pathway projections to the GPe, focusing on CB1 and $GABA_B$ receptor modulation. We validated a slice photometry approach to measure presynaptic Ca^{2+} at iSPN-GPe projections, using transgenic mice expressing the Ca^{2+} indicator GCaMP6f in iSPNs. We also used transgenic mice expressing the excitatory opsin channelrhodopsin (hChR2) to study the mechanisms regulating CB1 and $GABA_B$ effects on GABAergic transmission at iSPN-GPe synapses. We found that P/Q-type VGCCs are the primary VGCCs mediating presynaptic calcium and GABAergic transmission at iSPN synapses in the GPe. N- and L-type VGCCS contributed to control GABAergic transmission but not PreCaTs. GABAB receptor activation decreased presynaptic Ca^{2+} entry and GABAergic transmission. Conversely, CB1 receptor activation at iSPN projections did not decrease PreCaTs, while reducing GABAergic transmission. CB1 effects persisted when K_V1 and Na_V channels were blocked, and reduced the frequency of miniature inhibitory postsynaptic currents, suggesting a K_V1, Na_V and VGCC- independent mechanism of CB1 receptor inhibition of GABA release at iSPN terminals.

Methods

Animals

Experiments were conducted in accordance with the National Institutes of Health's Guidelines for Animal Care and Use, and all experimental procedures were approved by the National Institute on Alcohol Abuse and Alcoholism Animal Care and Use Committee. Mice were housed in groups of 2-4 in the NIAAA vivarium on a 12 hr light cycle with ad libitum access to food and water. B6;129S-Gt(ROSA)26Sortm95.1(CAG-GCaMP6f)Hze/J (GCaMP6f) and B6.Cg-Gt(ROSA)26Sortm32(CAG-COP4*H134R/EGFP)Hze/J (Ai14-ChR2) mice were purchased from The Jackson Laboratory (JAX; Bar Harbor, ME, USA). B6.FVB(Cg)-Tg(Adora2a-cre)KG139Gsat/Mmucd (A2A-Cre) mice were purchased from the Mutant mouse resource and research centers (MMRRC, 030869, Davis, CA, USA). These mutant mouse lines were maintained by breeding with wildtype C57BL6J mice purchased from JAX. Experimental animals were generated by breeding male or female mice homozygous for the GCaMP6f or ChR2 allele with mice heterozygous for the A2A-Cre alleles to restrict GCaMP6f or ChR2H134R (hChR2) expression to striatal indirect pathway SPNs. Male and female mice (aged 3-20 weeks) were included in the experiments. Genotyping was performed by polymerase chain reaction (PCR) on genomic DNA from ear biopsies.

Immunohistochemistry and confocal imaging

A2aGCaMP6 f mice (n = 3), were anesthetized with pentobarbital (50 mg/ kg) prior to the transcardiac perfusion of 1x PBS, followed by 4% formaldehyde (FA) (4% paraformaldehyde in 1x PBS). Brains were kept in 4% FA

overnight and then transferred to 1x PBS until slicing. Free-floating sections (50 mM) were cut using a Pelco easySlicer Vibratome (Ted Pella Inc., Redding, Ca, USA). Slices were washed 3 x 5 minutes in 1x PBS, and then incubated in a blocking solution containing 5% normal goat serum in PBS-T (0.2% Triton X-100). Slices were then incubated for 48 hr at 4C in 1x PBS containing the primary antibodies (Chicken anti-GFP, AbCam cat. No. #13970. 1:2000; Rabbit anti-NeuN, Cell Signaling Technology, cat. No. #24307, 1:1000). Slices were then washed 3 x 5 minutes in 1x PBS and incubated in 1x PBS containing the secondary antibodies for 2 hours (Alexa Fluor 488, Goat-anti-chicken, Invitrogen A11039, 1:500; Alexa Fluor 594 goat anti-rabbit, Invitrogen A11012, 1:500). A final wash of 3 x 5 minutes was performed prior to mounting using DAPI Fluoromount-G® (Southern Biotech, Cat No. 0100-20). Slices were imaged on a Zeiss LSM 800 laser confocal scan head mounted on a Zeiss Z1Axio Observer inverted microsope frame (Carl Zeiss, Oberkochen, Germany). An argon was used for 488 excitation (Alexa Fluor 488, dichroic MBS 488/594, emission 497-590), a HeNe594 laser for 594 excitation (Alexa Fluor 594, dichroic MBS 488/561, emission 598-670). Objectives used for imaging included a C-Apochromat 63x/1.2 NA W Korr M27 (Zeiss) and Plan-Apochromat 20x/0.8 NA.

Brain slice preparation for slice photometry and patch-clamp experiments

Mice were anesthetized with isoflurane and decapitated after assessing deep anesthesia by tail-pinch. The brain was rapidly collected and transferred to a slicing chamber filled with ice-cold sucrose-based cutting solution containing the following (in mM): 194 sucrose, 30 NaCl, 4.5 KCl, 26 $NaHCO_3$, 1.2 NaH_2PO_4, 10 D -glucose, 1 $MgCl_2$, saturated with 95% O_2/5% CO_2. Coronal sections (250-300 µm) containing the GPe/SNr were obtained using a Leica VT1200S Vibratome (Leica Microsystems, Buffalo Grove, IL) and rapidly moved to an incubation chamber filled with artificial cerebrospinal fluid (aCSF) containing (in mM): 124 NaCl, 4.5 KCl, 26 $NaHCO_3$, 1.2 NaH_2PO_4, 10 D-glucose, 1 $MgCl_2$, and 2 $CaCl_2$, saturated with 95% O_2/5% CO_2. Slices were incubated for 30-60 minutes at 32°C and then maintained at room temperature prior to recording. The same slicing protocol was used for slice photometry and patch-clamp experiments.

Slice photometry

Photometry recordings were acquired using a Zeiss upright epifluorescence microscope equipped with a 40x/0.8 NA water immersion objective. Slices were placed in a recording chamber and superfused at ~2 mL min-1 with aCSF warmed to ~30°C. GCaMP6f was excited using either a mercury HBO lamp, gated with a uniblitz shutter (Vincent Associates, Rochester, NY, USA) or a 470 nm LED (ThorLabs, Newton, NJ, USA) and filtered at 470 ± 20 nm. Excitation power was measured at the sample plane using a microscope slide photodiode power sensor (ThorLabs) and was 3.8 mW for the mercury HBO lamp and <1.0 mW for the 470 nm LED. Emitted light was collected and filtered at 525 ± 25 nm, passed through a 180 µm2 diaphragm and directed to a photomultiplier tube (PMT; Model D-104, Photon Technology International, Edison, NJ, USA). The PMT output was filtered at 1 kHz and digitized at 6.67 kHz using a Digidata 1322A and Clampex pClamp 10.6 software (Axon Instruments, Molecular Devices LLC, Sunnyvale, CA, USA). A bipolar stimulating electrode was placed in the lateral GPe, just inside the border between the striatum and GPe, and the 180 μm^2 field of view was positioned just lateral to the electrode tip. Photometry sweeps were acquired every 30 seconds. During each sweep, after an initial rapid decay in fluorescence, a presynaptic calcium transient was evoked by a train of 4 electrical pulses at 10Hz. Slices were equilibrated to the recording chamber conditions and electrical stimulation for ~20 min to allow for response stabilization. Photometry sweeps were averaged over 2 minutes (4 sweeps) before calculating peak ΔF/F values for electrically evoked presynaptic calcium transients (PreCaTs). For experiments using the mercury HBO lamp, the baseline fluorescence intensity tended to decay throughout the entire sweep so a baseline correction procedure was employed as described previously (Kupferschmidt and Lovinger, 2015). However, for experiments using the LED, the baseline fluorescence intensity tended to stabilize prior to evoking presynaptic calcium transients so the baseline correction procedure was omitted.

Whole-cell patch-clamp recordings

Hemislices were transferred to a recording chamber perfused with aCSF at 30–32 °C with a ~2 ml/min flow rate. Neurons were visualized with an upright microscope (Scientifica, Uckfield, East Sussex, UK) using a LUMPlanFL N × 40/0.80 NA W objective (Olympus, Waltham, MA). Recordings from GPe neurons were obtained using micropipettes (2–4 MΩ) made from 1.5 mm OD/1.12 mm ID borosilicate glass with a filament (World Precision Instruments, Sarasota, FL) pulled with a P-97 puller (Sutter Instruments Novato, CA). Micropipettes were filled with an intracellular solution containing the following (in mM): 150 CsCl, 10 HEPES, 2.0 $MgCl_2$, 0.3 Na-GTP, 3.0 Mg-ATP, 0.2 BAPTA-4Cs, 5 QX-314. Recordings were performed using a Multiclamp 700A amplifier and a Digidata 1322A or Multiclamp 700B and a digidata 1550B digitizer using a low-pass filter of 2 kHz and a sampling

frequency of 10 kHz. Data were analyzed using pClamp 10.3 or pClamp 10.6 software (Molecular Devices, Sunnyvale, CA). Recordings were obtained in voltage clamp mode. $GABA_A$ mediated spontaneous (sIPSCs) and optically evoked (oIPSCs) were isolated through the bath-perfusion of aCSF containing the AMPA receptor blocker DNQX (10 μM) and NMDA receptor blocker DL-AP5 (50 μM) and abolished by Gabazine application. To evoke IPSCs we used a train of 4 pulses at 10 Hz (pulse width 0.4 ms) every 30 seconds, using an optical stimulus at 470 nm (through a 4-channel LED driver, ThorLabs, MD, USA). To monitor series resistance (<30 MΩ) throughout the recording a 10mV, 50-100 ms depolarizing step was applied every minute; cells were excluded if the series resistance varied >20% during the recording.

Drugs

Stocks of ω-conotoxin GVIA, ω-agatoxin IVA, (R)-Baclofen, DNQX disodium salt, TTX, 4-AP and DL-AP5 sodium salt were dissolved in ddH2O. WIN55,212-2 mesylate and nifedipine were dissolved in 100% DMSO. All drug stocks were stored at -20°C and diluted in aCSF just prior to superfusion. QX-314 bromide was dissolved fresh in internal solution. ω-conotoxin GVIA and ω -agatoxin IVA were purchased form Alomone Labs (Jerusalem, Israel), QX-314 bromide and 4-AP from Millipore Sigma (St. Louis, MO, USA), and all other drugs from Tocris Biosciences (Minneapolis, MN, USA).

Statistical Analysis

Statistical analysis was performed in GraphPad Prism (GraphPad Software, La Jolla, California) and Excel. Significance was set at $p < 0.05$ in all analyses. All data are reported as mean + SD. Exact P values for all comparisons are reported in the main text and all figure legends. Statistical significance is indicated in the figures and figure legends. For all photometry and electrophysiology experiments, except for sIPSC and mIPSC experiments, the data are expressed as % of baseline (defined as the average of the last 8 - 10 minutes recorded prior to drug application). One-way rmANOVA with no correction followed by Tukey's multiple comparisons test was performed in experiments where 3 time points were compared (baseline: average of minute 3-8 of baseline; drug: last 2 minutes of drug application, washout: last 2 minutes of washout). Two-way rmANOVA with no correction followed by Tukey's multiple comparisons test was performed to compare the effects of application of different VGCC blockers on PreCaTs and oIPSCs. Experiments where 2 time points (baseline, drug) were compared were analyzed using paired t-test, normality distribution was assessed through the Shapiro-Wilk test.

Results

An optogenetic strategy to study presynaptic calcium transients and GABAergic transmission at indirect pathway projections to the GPe

To study presynaptic calcium and GABAergic transmission at iSPN-GPe projections we crossed Adora2a -Cre (A2a-Cre) mice with either GCaMP6f mice or AiCOP4 mice to express GCaMP6f or hChR2 in iSPNs. We imaged EYFP fluorescence in the A2a-AiCOP4 mice and found high expression in the dorsal striatum, GPe, but not in the SNr (Fig. 1A). Using immunohistochemistry, we quantified the percentage of striatal neurons expressing GCaMP6f in the A2aCre-GCaMP6f mice. We labeled neurons using the pan-neuronal marker NeuN and GFP to visualize GCaMP6f- expressing cells and found that on average of 3 mice, 43.55 % of striatal neurons expressed GFP (n = 3 animals, 5 micrographs/ mouse; n cells expressing GFP/ n of cells expressing GFP/ mouse: 461/1021, 396/1064, 486/1050), indicating GCaMP expression in ~half of the striatal SPNs (Fig. 1B). No GCaMP6f- expressing cell somata were found in the GPe, and sparse labeling was observed in the cortex.

We next functionally assessed the A2a-AiCOP4 line by performing whole-cell patch clamp recordings in the GPe. We used a low-chloride intracellular solution and first optogenetically stimulated the slice while clamping the membrane potential near the sodium reversal potential (~0mV). The outward current recorded at this holding potential was decreased by Gabazine to 5.9 + 3.2 % of baseline (Fig. 1C) (n=5 cells, 2 mice, paired t-test $p < 0.0001$). Next, we clamped the neurons near the chloride reversal potential (~ -45 mV) and recorded no current at this potential. We concluded that blue light stimulation of hChR2 expressing terminals in the A2aCre-AiCOP4 lines only evokes GABA release. Taken together, these validation steps indicated that the A2aCre-GCaMP6f and A2aCre-AiCOP4 lines represent a bona fide approach to study presynaptic calcium and GABA release from iSPN to GPe neurons.

We next tested whether the PreCaTs evoked in the GPe through local electrical stimulation (details in methods) were activity- dependent and Ca^{2+} dependent. In the first experiment, we delivered stimuli of increasing intensity using 100 μA increments (range 0 μA- 700 μA) and found that the PreCaTs amplitude increased with stimulation intensity, indicating its activity-dependence (Fig. 1D) (n = 5, one-way rmANOVA, $F_{(7,28)} = 26.7$, $p < 0.0001$). In

the second experiment, we followed the PreCaTs amplitude during a baseline period of 10 minutes, and next we switched the recording solution from normal ACSF to Ca^{2+}-free ACSF. The PreCaT amplitude decreased to 29.10 + 7 % of baseline during Ca^{2+}- free ACSF application, and re-application of normal ACSF partially restored the PreCaTs to 50.77 + 12.5 % of baseline (Fig. 1E) (n = 5 slices, one-way rmANOVA, Treatment: $F_{(2,8)} = 71.94$; $p < 0.0001$; Ca^{2+} free vs baseline $p < 0.0001$, washout vs Ca^{2+} free $p = 0.0186$, washout vs baseline $p < 0.0001$).

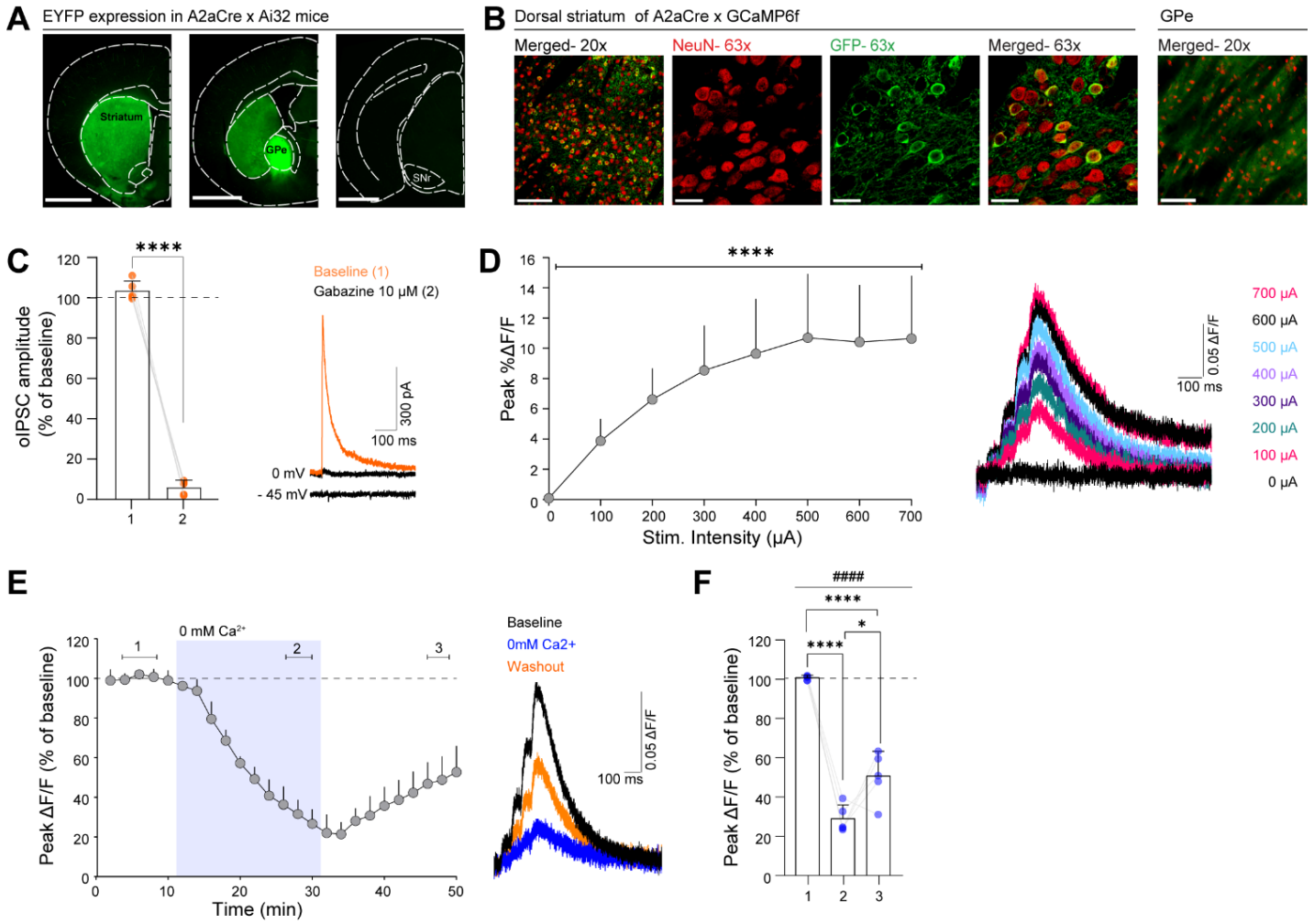

Figure 1. An optogenetic strategy to study presynaptic calcium transients and GABAergic transmission at indirect pathway projections to the GPe **A**: representative micrographs of EYFP expression in the A2aCre-AiCOP4 line. From left to right: coronal slices containing the dorsal striatum, GPe, SNr. Dense EYFP fluorescence was observed in the striatum and GPe, not in the SNr. B: representative confocal micrographs where IHC staining was performed in A2aCre-GCaMP6f mice using anti-GFP (green) and anti-NeuN (red). From left to right: 20x micrograph of dorsal striatum (scale bar: 100 µM); 63x micrographs of NeuN, GFP and the two channels merged in the dorsal striatum (scale bar: 25µM); 20x micrograph of GPe (scale bar: 100 µM). **C:** summary bar graph and example traces of whole-cell patch clamp experiments. Gabazine fully inhibited the currents recorded at iSPN-GPe synapses indicating their $GABA_A$ dependency (n = 5 cells). **D:** I/O curve experiment. The amplitude of the PreCaTs scaled with stimulation intensity indicating its activity-dependence (n = 5 slices). **E,F :** Time course of Ca^{2+} free ACSF application effects on PreCaTs. **E:** Summary of effects: baseline, last 2 minutes of Ca^{2+} free ACSF, last 2 minutes of washout. * P < 0.05; ** P < 0.001; *** P < 0.0001 ****/ #### P < 0.0001.

P/Q-type are the predominant VGCC controlling presynaptic Ca^{2+} and GABAergic transmission at the indirect pathway projections to the GPe

We designed a series of experiments to characterize the VGCCs mediating PreCaTs and GABAergic transmission at iSPN-GPe projections. First, we studied the effects of bath application of selective blockers of P/Q type, N-type or L-type VGCCs on PreCaTs (Fig. 2A, B). Application of the P/Q-type VGCC blocker, ω-agatoxin IVA (ATX, 200 nM), produced a decrease in PreCaTs amplitude to 71.72 + 12.73% of baseline and 53.28 + 18. 47 from baseline after washout (n = 6, one-way rmANOVA, Treatment: $F_{(2, 10)} = 32.53$; $p < 0.0001$;

drug vs baseline p = 0.0017, washout vs drug p = 0.0266, washout vs baseline p < 0.0001). Application of the N-type VGCC blocker, ω-Conotoxin GVIA (CTX, 1 μM), did not produce a significant decrease in PreCaTs amplitude, which was 85.24 + 11.29% of baseline after drug and 78.04 + 17.34 following washout (n = 8, one-way rmANOVA, Treatment: $F_{(2, 14)} = 8.38$; p = 0.004; drug vs baseline p = 0.0565, washout vs drug p = 0.322, washout vs baseline p = 0.0032). Bath application of the L-type VGCC blocker, Nifedipine (10 μM), did not decrease PreCaTs amplitude at iSPN-GPe projections, which was 94.97 + 5.6% of baseline and 90.24 + 7.77 after washout (n= 5, one-way rmANOVA, Treatment: $F_{(2, 8)} = 3.638$, P = 0.0752). Two-way rmANOVA comparison of Agatoxin, Conotoxin and Nifedipine application effects on PreCaTs at iSPN-GPe projections revealed a significant interaction between the time (timepoints analyzed: baseline, drug, washout) and drug factors, indicating a difference in the effect of the 3 blockers on PreCaTs (Time X drug: $F_{(4, 32)} = 6.933$; p = 0.0004; agatoxin vs nifedipine p = 0.004). Overall, these results indicate that P/Q type VGCCs are the primary controllers of PreCaTs at iSPN-GPe terminals.

Next, we examined the effects of the bath application of selective blockers of P/Q type, N-type or L-type VGCCs on GABAergic transmission (Fig. 2C, D). Application of ATX, induced a decrease in oIPSC amplitude to 20.15 + 14.38% of baseline which persisted at 8.64 + 7.2% of baseline after washout (iSPN-GPe, one-way rmANOVA, n = 5, Treatment: $F_{(2, 8)} = 189.1$; p < 0.0001; drug vs baseline p < 0.0001, washout vs drug p = 0.11, washout vs baseline p < 0.0001). Application of CTX induced a significant decrease in oIPSC amplitude to 73.21 + 12.71% of baseline which persisted at 69.09 + 22.57 after washout (n = 5, one-way rmANOVA, Treatment: $F_{(2, 8)} = 8.4$; p = 0.0108; drug vs baseline p = 0.0275, washout vs drug p = 0.8689, washout vs baseline p = 0.0133). Application of Nifedipine induced a significant decrease in oIPSC amplitude to 78.91 + 11.12% of baseline which persisted at 80.59 + 12.88 after washout (n= 5, one-way rmANOVA, Treatment: $F_{(2, 8)} = 10.97$, P = 0.0051; drug vs baseline p = 0.0074, washout vs drug p = 0.9437, washout vs baseline p = 0.0115). Two-way RM ANOVA comparison of ATX, CTX and Nifedipine application effects on oIPSCs at iSPN-GPe synapses revealed a significant interaction between the time (timepoints analyzed: baseline, drug washout) and drug factors (Time X drug: $F_{(4, 24)} = 21.09$; p < 0.0001; agatoxin vs conotoxin p < 0.0001, agatoxin vs nifedipine p < 0.0001). Taken together, these results indicate that P/Q type VGCCs are the primary VGCC involved in GABAergic transmission at iSPN-GPe synapses, most likely due to a role in GABA release. In contrast, N-type and L-type VGCCs play a significant but smaller role.

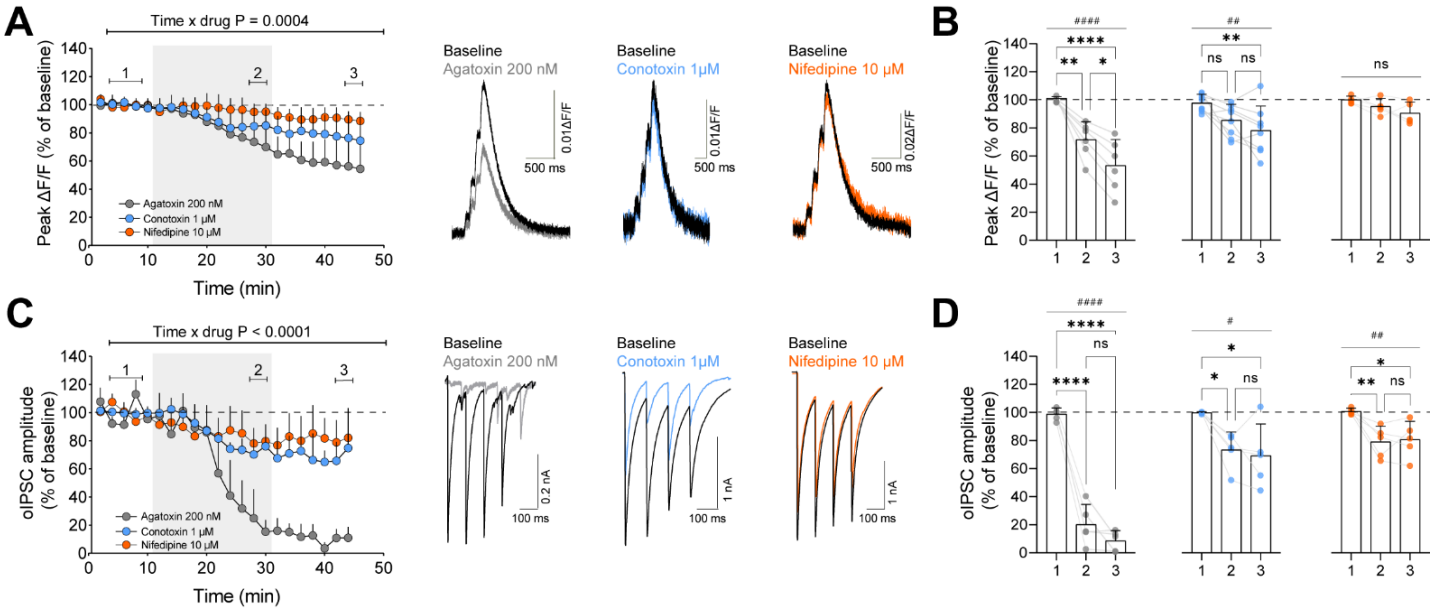

Figure 2: P/Q-type are the predominant VGCC controlling presynaptic Ca^{2+} and GABAergic transmission at the indirect pathway projections to the GPe. A: Timecourse of VGCC blocker application effects on PreCaTs and raw photometry traces. B: Summary of drug effects: baseline, last 2 minutes of drug, last 2 minutes of washout. Blockade of P/Q -type VGGCs (Agatoxin, n = 6 slices) significantly decreased PreCaTs from baseline, whereas no significant effect on PreCaTs was observed by blocking N-type VGCCs (Conotoxin, n= 8 slices) or L-type VGCCs (Nifedipine, n = 5 slices). C: Timecourse of VGCC blocker application effects on oIPSCs and raw electrophysiological traces. D: Comparison of drug effects: baseline, last 2 minutes of drug, last 2 minutes of washout. Blockade of P/Q -type VGGCs (Agatoxin, n = 5 cells)

significantly decreased PreCaTs from baseline, and smaller but significant effects were induced by blocking N-type VGCCs (Conotoxin, n = 5 cells) or L-type VGCCs (Nifedipine, n = 5 cells). * p < 0.05; **/ ## P < 0.01; *** P < 0.0001; ****/ #### P < 0.0001.

VGCC-dependent modulation of iSPN-GPe projections by $GABA_B$ receptors

We studied the effects of $GABA_B$ receptor activation on PreCaTs at iSPN-GPe projections (Fig. 3A, B). Bath application of the $GABA_B$ agonist Baclofen (10 µM) decreased PreCaTs amplitude to 45.73 + 15.13% of baseline which persisted at 50.81 + 23.25% of baseline after washout (n = 7, one-way rmANOVA, Treatment: $F_{(2, 12)}$ = 40.94; p < 0.0001; drug vs baseline p < 0.0001, washout vs drug p = 0.7323, washout vs baseline p < 0.0001). To test whether Baclofen application induced a long-term depression of PreCaTs at iSPN-GPe projections we performed a second experiment of pulse-chase where following Baclofen we bath applied the $GABA_B$ antagonist CGP 35358 (2 µM) (Fig. 3C, D). Bath application of Baclofen decreased PreCaTs amplitude to 46.52 + 12.65% of baseline, an effect that was reversed by CGP 35358 which brought PreCaTs to 107.5 + 23.05% of baseline (n = 5, one-way rmANOVA, Treatment: $F_{(2, 8)}$ = 23.10; p = 0.0005; drug vs baseline p = 0.0014, washout vs drug p = 0.0007, washout vs baseline p = 0.7848).

We next examined effects of $GABA_B$ receptor activation on GABAergic synaptic responses at iSPN-GPe projections (Fig. 3E, F). Bath application of the $GABA_B$ agonist Baclofen decreased the oIPSC amplitude to 49.77 + 15.96% of baseline (n = 7, paired t-test, p = 0.0002). To determine the site of action of $GABA_B$ receptors in the GPe we analyzed sIPSCs (Fig. 3G). We found that Baclofen application induced a significant decrease in sIPSC frequency from baseline 3.963 + 1.32 to Baclofen 2.282 + 2.707 Hz and amplitude from baseline 55.72 + 25.36 to Baclofen 47.06 + 22.07 pA (Frequency: n = 12, paired t-test, p = 0.0195; Amplitude: n = 12, paired t-test, p < 0.0001). The observed sIPSC decrease induced by baclofen application is indicative of a presynaptic effect, whereas a change in amplitude might reflect an effect on multivesicular release or a shift in the population of synapses contributing to the sIPSCs. Taken together, these experiments indicate that $GABA_B$ receptor modulation of iSPN-GPe projections is reversible, VGCC- mediated and involves presynaptic modulation of GABA release.

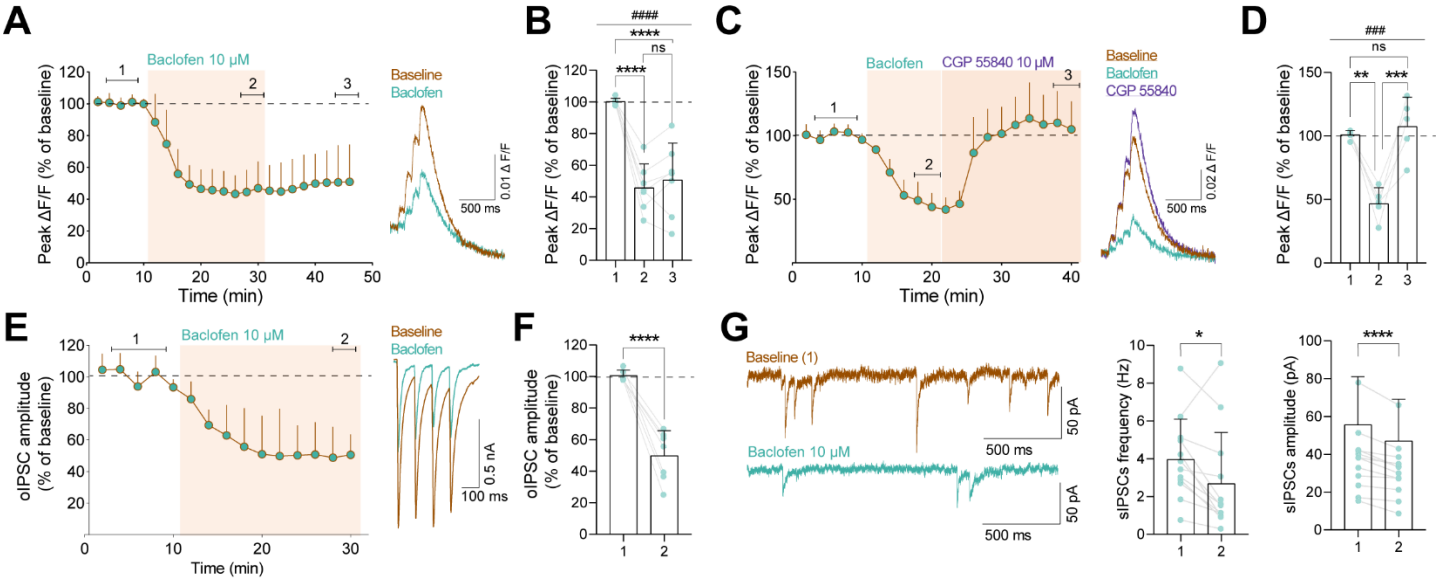

Figure 3: VGCC-dependent modulation of iSPN-GPe projections by GABAB receptors. A: Time course of Baclofen effects on PreCaTs and raw photometry traces. **B:** Summary of drug effects: baseline, last 2 minutes of drug, last 2 minutes of washout. $GABA_B$ activation (Baclofen, n = 7 slices) significantly decreased PreCaTs amplitude. **C:** Time course experiment of Baclofen followed by CBP 55840 effects on PreCaTs **D:** Baclofen significantly decreased PreCaTs and CGP55840 application reversed PreCaTs to baseline levels (n = 5 slices). **E:** Time course of Baclofen effects on oIPSCs at iSPN-GPe synapses and raw electrophysiological traces. **F:** Baclofen significantly reduced oIPSCs at iSPN-GPe terminals (n = 7 cells). **G:** Effects of Baclofen application on sIPSCs. Example traces and summary bar graphs. Baclofen application significantly decreased the frequency and amplitude of sIPSCs recorded in the GPe, indicating a pre-synaptic site of action (n= 12 cells). * p < 0.05; **/ ## P < 0.001; ***/ ### P < 0.001; ####/ **** P < 0.0001.

VGCC- and K_V1- independent mechanisms of presynaptic modulation of iSPN-GPe projections by CB1 receptors

We next studied the effects of CB1 receptor activation on PreCaTs at iSPN-GPe projections (Fig. 4 A, B). Bath application of the CB1 agonist WIN 55212-2 did not change PreCaTs amplitude, which was 100.3 + 19.68% of baseline following WIN 55212-2 (WIN) application and 86.58 + 15.74 after washout (n = 7, one-way rmANOVA, Treatment: $F_{(2, 8)} = 2.386$; p = 0.1539). CB1 receptors are densely expressed in the GPe and their activation has been previously shown to reduce GABA release in this brain region (Engler et al., 2006), therefore we first asked whether CB1 receptors reduced GABAergic transmission specifically at iSPN-GPe synapses (Fig. 4C, D. Bath application of WIN decreased the oIPSC amplitude to 47.82 + 20.77 from baseline (n = 5, paired t-test, p = 0.0053). Considering that CB1 activation did not decrease PreCaTs while inhibiting GABAergic transmission at iSPN-GPe projections we designed a series of experiments to test for VGCC-independent effects of CB1 receptors at these synapses. First, we recorded mIPSCs in the presence of the NaV blocker TTX (Fig. 4E). Bath application of WIN 55212-2 decreased the mIPSC frequency from 1.967 + 1.4 to 1.394 + 0.88 Hz (n = 7, p = 0.0312) and decreased the mIPSC amplitude from 44.28 + 13.59 to 31.13 + 6.488 pA (n = 7, p = 0.0250). This indicates a presynaptic effect of CB1 receptor activation on GABA release in the GPe, but a change in amplitude might be indicative of an additional postsynaptic contribution, an effect on multivesicular release or a shift in the population of synapses contributing to the mIPSCs. Additionally, as mIPSCs occur in the absence of action potential/ Ca^{2+} influx mediated release events, these results also indicate a VGCC-independent action of CB1 receptors in the GPe. We speculated that CB1 receptor effects at iSPN-GPe synapses might be mediated by KV1 channels, that have been proposed to mediate CB1 effects at other synapses. Hence, we recorded oIPSCs evoked in the presence of TTX and the KV1 blocker 4-AP (Fig. 4 F, G). We found that WIN 55212-2 application produced a reduction of oIPSCs amplitude to 52.25 + 22. 49% of baseline (n=4, paired t-test, p = 0.0216) under these conditions. These experiments indicate that CB1 effects are independent of the inhibition of K_V1 channels on iSPN-GPe projections. Taken together, these experiments indicate that presynaptic modulation of iSPN-GPe projections by CB1 receptors occurs through a mechanism independent of the inhibition of presynaptic VGCCs.

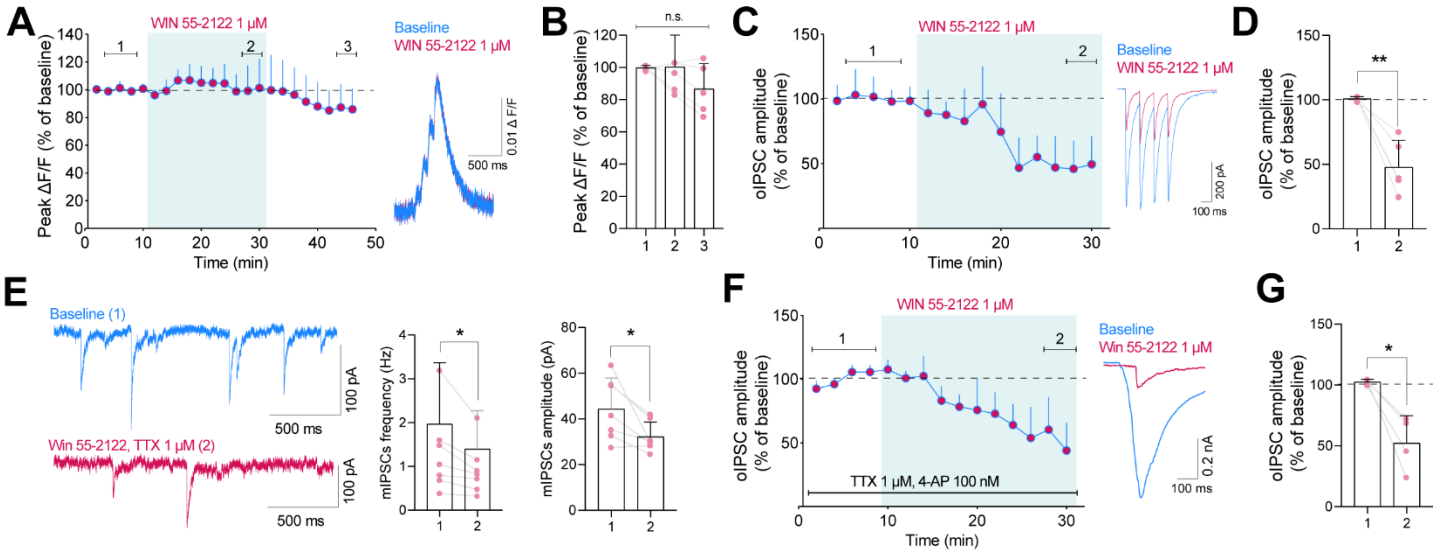

Figure 4: VGCC- and KV1-independent mechanisms of presynaptic modulation of iSPN-GPe projections by CB1 receptors. Time course of WIN effects on PreCaTs and raw photometry traces. **B:** Summary of drug effects: baseline, last 2 minutes of drug, last 2 minutes of washout. CB1 receptor activation (WIN 55-2122, n = 7 slices) did not change PreCaTs amplitude. **C:** Time course of WIN effects on oIPSCs at iSPN-GPe synapses and raw electrophysiological traces **E:** WIN 55-2122 application significantly decreased oIPSC amplitude (n = 5 cells). **E:** Time course of WIN 55-2122 effects on oIPSCs recorded in the presence of TTX + 4AP. **F:** WIN 55-2122 significantly reduced oIPSCs at iSPN-GPe terminals (n = 7 cells). **G:** Effects of WIN 55-2122 application on mIPSCs. Example traces and summary bar graphs. WIN 55-2122 application significantly decreased the frequency and amplitude of mIPSCs (n= 7 cells). * p < 0.05; ** P < 0.011.

Discussion

Here we used a combination of brain slice photometry and whole-cell patch clamp to study the presynaptic modulation of indirect pathway projections (iSPN-GPe) by CB1 and $GABA_B$ receptors. We first determined that presynaptic calcium and GABA release at striatal iSPN-GPe terminals are primarily mediated by P/Q-type VGCCs. $GABA_B$ receptors modulate presynaptic Ca^{2+} and GABA release at these terminals through a presynaptic mechanism. CB1 receptors control GABA release but not presynaptic Ca^{2+} through a VGCC-, NaV and KV1 independent presynaptic mechanism. These findings support the idea that $GABA_B$ and CB1 receptors mediate presynaptic inhibition at these synapses through distinct mechanisms.

We studied presynaptic Ca^{2+} at iSPN-GPe projections using a genetic approach to express GCaMP6f in iSPNs that give rise to the indirect pathway striatal projections. As a result, GCaMP6f was expressed in iSPNs independent of their location in striatal subregions (DMS, VMS and DLS) or the molecularly defined striatal subcompartments, patch and matrix. Using field photometry and pharmacology we were able to measure activity-dependent presynaptic Ca^{2+} transients and determine which VGCCs subtypes mediated them, as well as their modulation by $GABA_B$ and CB1 receptors. Field photometry allowed the measurement of presynaptic Ca^{2+} in a selected field of view within the GPe containing iSPN axons. This population-level measurement likely reflects the sum of axonal Ca^{2+} proximal to, and distal from, presynaptic terminals/ release sites given the widespread expression of the fluorescent indicator throughout the axon. Ultimately, the spatial resolution of field photometry might not be sufficient to reflect small Ca^{2+} variations restricted to the presynaptic terminals but critical for neurotransmitter release. To counter this limitation, we generated mice genetically expressing hChR2 in iSPNs and performed patch-clamp recordings to measure neurotransmitter release with high temporal and spatial resolution at iSPN-GPe projections. The use of whole cell patch-clamp allowed us to study activity- dependent neurotransmitter release and its control by VGCCs, $GABA_B$ and CB1 receptors. It also allowed the measurement of action potential-independent, VGCC-independent neurotransmitter release by recording mIPSCs in the presence of the NaV blocker TTX. Taken together, a combination of field photometry and whole cell patch-clamp combined with optogenetics allowed us to gain mechanistic insights on the modulation of iSPN projections by GPCRs. It is possible that small variations in presynaptic Ca^{2+}, which we did not detect using slice photometry, contribute to the small but significant reduction in GABA release induced by the antagonism of N-type and P/Q type VGCCs.

Our results indicate that CB1 receptors modulate iSPN-GPe projections by reducing GABA release while our slice photometry experiments indicated no effect of CB1 receptor activation on presynaptic Ca^{2+}. We measured NaV and VGCC-independent GABA release by including the NaV blocker TTX (mIPSCs) in the extracellular solution and found that the effects of CB1 receptor activation on GABA release persisted. Further, the effects of CB1 receptor activation on GABA release were observed in recordings were TTX and the KV1 antagonist 4-AP were included. Overall, our presynaptic Ca^{2+} measurements and neurotransmitter release measurements converged in indicating a VGCC-independent, KV1 independent modulatory action of CB1 receptors on iSPN terminals in the GPe. These results reproduce, extend, and provide synapse specificity to previously published work on the inhibitory effect of CB1 receptors on GABAergic synaptic transmission in the GPe (Engler et al., 2006). CB1 receptors have been proposed to suppress neurotransmitter release through the activation of KV channels at cortico-accumbal (Robbe et al., 2001) and cerebellar parallel fiber synapses (Daniel et al., 2004). CB1-mediated inhibition of NaV-independent GABA release in the dorsal striatum was also observed (Adermark et al., 2009). Other studies proposed that presynaptic CB1 receptors depress glutamate release at cortico-dorsal striatum synapses through the inhibition of N-type Ca^{2+} channels (Huang et al., 2001), and a similar VGCC-dependent action was reported at hippocampal GABAergic synapses (Hoffman & Lupica, 2001). CB1 receptors depress presynaptic Ca^{2+} influx at cerebellar granule-Purkinje cell synapses (Brown et al., 2004), as well as Ca^{2+} currents at calyx of Held synapses in the auditory brainstem (Kushmerick et al., 2004). The signaling cascade recruited by CB1 receptor activation on iSPN-GPe terminals remains to be fully elucidated. A possible alternative might involve the direct interaction of the $G_{B\gamma}$ subunit with SNARE complexes. It has been proposed that $G_{B\gamma}$ subunits can target the C-terminus domain of SNAP-25 (Zurawski et al., 2019). This mechanism has been documented to mediate effects of 5HT1B effects in the hippocampus, α2a adrenergic receptor on glutamatergic synapses in the BNST, (Zurawski et al., 2019), and $GABA_B$ receptors on glutamatergic inputs to SPNs in the nucleus accumbens (Manz et al., 2019). However, CB1 receptors have not yet been shown to activate this signaling cascade.

What is the functional significance of CB1 receptor signaling on iSPN-GPe terminals? The levels of the CB1 receptor in the GPe are among the highest in the CNS. The endocannabinoids anandamide and 2-arachidonoylglycerol (2AG) were detected in the rat GPe (Di Marzo et al., 2000) but the mechanisms driving their release remain unclear. Local GPe micronjections of synthetic cannabinoids were found to increase ipsilateral rotations (Sañudo-Peña et al., 1999) and to enhance muscimol-induced catalepsy (Pertwee & Wickens, 1991). Further, reserpine treatment enhanced anandamide and 2-AG levels in the rat GPe (Di Marzo et al., 2000). The motor effects of cannabinoids in the GPe might be mediated through effects on dSPN-GPe synapses and subthalamo-pallidal synapses in addition to the effects on iSPN-GPe synapses (Brotchie, 2003).

We found that $GABA_B$ receptors modulate the iSPN-GPe projection by suppressing GABA release and presynaptic Ca^{2+}. $GABA_B$ receptor activation decreased sIPSC frequency in the GPe, indicating a presynaptic site of action. A decrease in sIPSC frequency and amplitude does not exclude $GABA_B$ receptor-mediated inhibition of other GABAergic inputs to the GPe, including local collaterals and bridge collateral dSPN projections. A decrease in sIPSC amplitude might result from the inhibition of selected GABAergic inputs or from the reduction of multi-peak postsynaptic responses. These results are consistent with previous reports indicating VGCCs as one of the downstream targets of $GABA_B$ receptor signaling at corticostriatal synapses (Kupfershmidt & Lovinger, 2015) granule-Purkinje cell cerebellar synapses (Dittman & Regehr, 1996) and hippocampal synapses (Doze et al., 1995; Wu & Saggau, 1995). Ultrastructural studies have identified the site of expression of $GABA_B$ receptors in the GPe in rodents and primates (Charara et al., 1999; Chen et al., 2004). Pre-synaptic $GABA_B$ receptors were found on GABAergic inputs to the GPe and on anterogradely labelled striatopallidal projections. Further, $GABA_B$ receptors were found post-synaptically at GABAergic synapses and presynaptically at glutamatergic synapses in the GPe (Chen et al., 2004). Hence, $GABA_B$ receptors are positioned to regulate GPe physiology as autoreceptors, heteroreceptors or postsynaptic receptors. In our recording conditions, no $GABA_B$ mediated postsynaptic responses were observed since GIRK channels were blocked by including Cs^+ in the intracellular recording solution. Conversely, CB1 receptors in the GPe might be primarily recruited by endocannabinoids released retrogradely. Alternatively, astrocytes surrounding striatopallidal projections (Galvan et al., 2010) might provide an alternative source of endocannabinoids, although these remain untested hypotheses. In addition to CB1 and $GABA_B$ receptors being recruited through different synaptic mechanisms, we show that the two receptors involve distinct presynaptic signaling mechanisms. By inhibiting VGCCs, $GABA_B$ receptors might shunt action potential evoked neurotransmitter release at iSPN-GPe synapses, in response to increased presynaptic activity (autoreceptor role) or increased local GABA (heteroreceptor role). CB1 receptors might function synergistically with $GABA_B$ receptors by further decreasing GABA release from striatopallidal synapses. Alternatively, endocannabinoid production and release at iSPN-GPe synapses might be recruited by neuromodulatory or glutamatergic inputs to the GPe thus modulating iSPN-GPe inputs independently from iSPN firing activity.

The modulation of presynaptic function is a crucial step in controlling the efficacy of synaptic transmission in the brain. Past studies have identified the CB1 and $GABA_B$ receptors as important modulators of GPe function but lacked synapse specificity. The growing understanding of the GPe cell-type composition, connectivity, microcircuitry and function requires a synapse-specific approach to contextualize the role of CB1 and $GABA_B$ receptor signaling in this region. Here, we used a synapse-specific approach to focus on the iSPN-GPe projection. A detailed analysis of the striato-pallidal and pallido-pallidal circuitry has proposed that iSPN-GPe projections are the densest in the GPe and primarily target PV-expressing neurons over Npas1- expressing GPe neurons (Cui et al., 2021) and similar results in vivo have shown a preferential innervation of prototypic GPe neurons by iSPNs (Ketzef et al., 2021). In turn, PV+ neurons represent the primary source of collateral inhibition in the GPe (Cui et al., 2021; Higgs et al., 2021). Presynaptic inhibition of iSPN-GPe projections might therefore produce primarily a disinhibition of the output of GPe prototypic neurons to the SNr, STN and PF thalamus (Lilasharoen et al., 2020; Pamukcu et al., 2020) in addition to disinhibiting local collaterals. Functionally, presynaptic modulation of iSPN-GPe projections has implications for motor control and action selection. The indirect pathway has been implicated in motor suppression by classic models of basal ganglia circuit function (Grillner et al., 2016; Albin et al., 1989; Kravitz et al., 2010; Cui et al., 2021; Isett et al., 2022). Further, the indirect pathway has been proposed to be involved in negative reinforcement (Kravitz et al., 2012). Optogenetic dissection of the indirect pathway has revealed that the activation of striatal iSPNs has a locomotor-suppressing effect, an effect replicated in several studies where the optogenetic manipulation was performed in the dorsomedial striatum (Cui et al., 2021; Kravitz et al., 2010; Isett et al., 2022). Conversely, the inhibition of iSPNs in the dorsolateral striatum had movement promoting effects (Cui et al., 2021), although the underlying circuitry

remains unclear. Optogenetic somatic manipulations of iSPN activity will influence local iSPN collaterals in addition to downstream projections. A recent study suggests that when the optogenetic manipulation is titrated to only inhibit iSPN-GPe terminals no locomotor effects are observed while the negative reinforcing effects persist (Isett et al., 2022). The presynaptic modulation of iSPN-GPe projections is therefore important for movement and action selection and might play distinct roles on functionally distinct iSPN-GPe projections from the dorsomedial and dorsolateral striatum.

In conclusion, our results suggest that distinct mechanisms of presynaptic modulation are recruited by CB1 and $GABA_B$ receptors on the striatal indirect pathway projections to the GPe. Presynaptic modulation by CB1 and $GABA_B$ receptors decrease the synaptic efficacy of iSPN-GPe projections, a function that might be recruited by distinct functional states in the GPe and ultimately contribute to shape the basal ganglia output. Our results encourage research on the synapse-specific mechanisms of Gi/o coupled receptor signaling which might inform the development of targeted pharmacological treatments for movement and psychiatric disorders.

Author contributions

KPA, DL, GS and DML were responsible for the conception and design of the study. KPA, DL, GS performed electrophysiological recordings. GS analyzed electrophysiological recordings. KPA, DL and GMC performed slice photometry experiments and analyses. GS performed and analyzed immunohistochemical experiments. GS drafted the manuscript and the figures with inputs from all authors and all authors gave final approval.

Acknowledgments

This work was supported by the National Institutes of Health, National Institute on Alcohol Abuse and Alcoholism, Division of Intramural Clinical and Biological Research (ZIAAA000416). We thank the NIAAA animal care stuff for their precious support for animal husbandry and veterinary care. We thank Guoxiang Luo for genotyping assistance, and all the Laboratory for Integrative Neurosciences for the helpful discussions.

Data availability statement

All data generated or analyzed in this manuscript are included in the manuscript and its supplementary file(s).

References

1. *Adermark, L., Talani, G., & Lovinger, D. M. (2009). Endocannabinoid-dependent plasticity at GABAergic and glutamatergic synapses in the striatum is regulated by synaptic activity. The European journal of neuroscience, 29(1), 32–41. https://doi.org/10.1111/j.1460-9568.2008.06551*
2. *Albin, R. L., Young, A. B., & Penney, J. B. (1989). The functional anatomy of basal ganglia disorders. Trends in neurosciences, 12(10), 366–375. https://doi.org/10.1016/0166-2236(89)90074-x*
3. *Araque, A., Castillo, P. E., Manzoni, O. J., & Tonini, R. (2017). Synaptic functions of endocannabinoid signaling in health and disease. Neuropharmacology, 124, 13–24. https://doi.org/10.1016/j.neuropharm.2017.06.017*
4. *Bonm, A. V., Elezgarai, I., Gremel, C. M., Viray, K., Bamford, N. S., Palmiter, R. D., Grandes, P., Lovinger, D. M., & Stella, N. (2021). Control of exploration, motor coordination and amphetamine sensitization by cannabinoid CB1 receptors expressed in medium spiny neurons. The European journal of neuroscience, 54(3), 4934–4952. https://doi.org/10.1111/ejn.15381*
5. *Borgkvist, A., Avegno, E. M., Wong, M. Y., Kheirbek, M. A., Sonders, M. S., Hen, R., & Sulzer, D. (2015). Loss of Striatonigral GABAergic Presynaptic Inhibition Enables Motor Sensitization in Parkinsonian Mice. Neuron, 87(5), 976–988. https://doi.org/10.1016/j.neuron.2015.08.022*
6. *Boyes, J., & Bolam, J. P. (2003). The subcellular localization of GABA(B) receptor subunits in the rat substantia nigra. The European journal of neuroscience, 18(12), 3279–3293. https://doi.org/10.1111/j.1460-9568.2003.03076.x*
7. *Brown, S. P., Safo, P. K., & Regehr, W. G. (2004). Endocannabinoids inhibit transmission at granule cell to Purkinje cell synapses by modulating three types of presynaptic calcium channels. The Journal of neuroscience : the official journal of the Society for Neuroscience, 24(24), 5623–5631. https://doi.org/10.1523/JNEUROSCI.0918-04.2004*
8. *Brotchie J. M. (2003). CB1 cannabinoid receptor signalling in Parkinson's disease. Current opinion in pharmacology, 3(1), 54–61. https://doi.org/10.1016/s1471-4892(02)00011-5*
9. *Chalifoux, J. R., & Carter, A. G. (2011). GABAB receptor modulation of synaptic function. Current opinion in neurobiology, 21(2), 339–344. https://doi.org/10.1016/j.conb.2011.02.004*

10. *Chang, H. T., Wilson, C. J., & Kitai, S. T. (1981). Single neostriatal efferent axons in the globus pallidus: a light and electron microscopic study. Science (New York, N.Y.), 213(4510), 915–918. https://doi.org/10.1126/science.7256286*
11. *Chen, L., Boyes, J., Yung, W. H., & Bolam, J. P. (2004). Subcellular localization of GABAB receptor subunits in rat globus pallidus. The Journal of comparative neurology, 474(3), 340–352. https://doi.org/10.1002/cne.20143*
12. *Charara, A., Heilman, T. C., Levey, A. I., & Smith, Y. (2000). Pre- and postsynaptic localization of GABA(B) receptors in the basal ganglia in monkeys. Neuroscience, 95(1), 127–140. https://doi.org/10.1016/s0306-4522(99)00409-1*
13. *Cui, Q., Pamukcu, A., Cherian, S., Chang, I., Berceau, B. L., Xenias, H. S., Higgs, M. H., Rajamanickam, S., Chen, Y., Du, X., Zhang, Y., McMorrow, H., Abecassis, Z. A., Boca, S. M., Justice, N. J., Wilson, C. J., & Chan, C. S. (2021). Dissociable Roles of Pallidal Neuron Subtypes in Regulating Motor Patterns. The Journal of neuroscience : the official journal of the Society for Neuroscience, 41(18), 4036–4059. https://doi.org/10.1523/JNEUROSCI.2210-20.2021*
14. *Daniel, H., Rancillac, A., & Crepel, F. (2004). Mechanisms underlying cannabinoid inhibition of presynaptic Ca2+ influx at parallel fibre synapses of the rat cerebellum. The Journal of physiology, 557(Pt 1), 159–174. https://doi.org/10.1113/jphysiol.2004.063263*
15. *Davis, M. I., Crittenden, J. R., Feng, A. Y., Kupferschmidt, D. A., Naydenov, A., Stella, N., Graybiel, A. M., & Lovinger, D. M. (2018). The cannabinoid-1 receptor is abundantly expressed in striatal striosomes and striosome-dendron bouquets of the substantia nigra. PloS one, 13(2), e0191436. https://doi.org/10.1371/journal.pone.0191436*
16. *Dittman, J. S., & Regehr, W. G. (1996). Contributions of calcium-dependent and calcium-independent mechanisms to presynaptic inhibition at a cerebellar synapse. The Journal of neuroscience : the official journal of the Society for Neuroscience, 16(5), 1623–1633. https://doi.org/10.1523/JNEUROSCI.16-05-01623.1996*
17. *Di Marzo, V., Hill, M. P., Bisogno, T., Crossman, A. R., & Brotchie, J. M. (2000). Enhanced levels of endogenous cannabinoids in the globus pallidus are associated with a reduction in movement in an animal model of Parkinson's disease. FASEB journal : official publication of the Federation of American Societies for Experimental Biology, 14(10), 1432–1438. https://doi.org/10.1096/fj.14.10.1432*
18. *Doze, V. A., Cohen, G. A., & Madison, D. V. (1995). Calcium channel involvement in GABAB receptor-mediated inhibition of GABA release in area CA1 of the rat hippocampus. Journal of neurophysiology, 74(1), 43–53. https://doi.org/10.1152/jn.1995.74.1.43*
19. *Engler, B., Freiman, I., Urbanski, M., & Szabo, B. (2006). Effects of exogenous and endogenous cannabinoids on GABAergic neurotransmission between the caudate-putamen and the globus pallidus in the mouse. The Journal of pharmacology and experimental therapeutics, 316(2), 608–617. https://doi.org/10.1124/jpet.105.092718*
20. *Galvan, A., Hu, X., Smith, Y., & Wichmann, T. (2010). Localization and function of GABA transporters in the globus pallidus of parkinsonian monkeys. Experimental neurology, 223(2), 505–515. https://doi.org/10.1016/j.expneurol.2010.01.018*
21. *Gerfen, C. R., Engber, T. M., Mahan, L. C., Susel, Z., Chase, T. N., Monsma, F. J., Jr, & Sibley, D. R. (1990). D1 and D2 dopamine receptor-regulated gene expression of striatonigral and striatopallidal neurons. Science (New York, N.Y.), 250(4986), 1429–1432. https://doi.org/10.1126/science.2147780*
22. *Graveland, G. A., & DiFiglia, M. (1985). The frequency and distribution of medium-sized neurons with indented nuclei in the primate and rodent neostriatum. Brain research, 327(1-2), 307–311. https://doi.org/10.1016/0006-8993(85)91524-0*
23. ***23** Grillner, S., & Robertson, B. (2016). The Basal Ganglia Over 500 Million Years. Current biology : CB, 26(20), R1088–R1100. https://doi.org/10.1016/j.cub.2016.06.041*
24. *Higgs, M. H., Jones, J. A., Chan, C. S., & Wilson, C. J. (2021). Periodic unitary synaptic currents in the mouse globus pallidus during spontaneous firing in slices. Journal of neurophysiology, 125(4), 1482–1500. https://doi.org/10.1152/jn.00071.2021*
25. *Hoffman, A. F., & Lupica, C. R. (2000). Mechanisms of cannabinoid inhibition of GABA(A) synaptic transmission in the hippocampus. The Journal of neuroscience : the official journal of the Society for Neuroscience, 20(7), 2470–2479. https://doi.org/10.1523/JNEUROSCI.20-07-02470.2000*
26. *Hu, S. S., & Mackie, K. (2015). Distribution of the Endocannabinoid System in the Central Nervous System. Handbook of experimental pharmacology, 231, 59–93. https://doi.org/10.1007/978-3-319-20825-1_3*

27. *Huang, C. C., Lo, S. W., & Hsu, K. S. (2001). Presynaptic mechanisms underlying cannabinoid inhibition of excitatory synaptic transmission in rat striatal neurons. The Journal of physiology, 532(Pt 3), 731–748. https://doi.org/10.1111/j.1469-7793.2001.0731e.x*
28. *Ketzef, M., & Silberberg, G. (2021). Differential Synaptic Input to External Globus Pallidus Neuronal Subpopulations In Vivo. Neuron, 109(3), 516–529.e4. https://doi.org/10.1016/j.neuron.2020.11.006*
29. *Kravitz, A. V., Tye, L. D., & Kreitzer, A. C. (2012). Distinct roles for direct and indirect pathway striatal neurons in reinforcement. Nature neuroscience, 15(6), 816–818. https://doi.org/10.1038/nn.3100*
30. *Kravitz, A. V., Freeze, B. S., Parker, P. R., Kay, K., Thwin, M. T., Deisseroth, K., & Kreitzer, A. C. (2010). Regulation of parkinsonian motor behaviours by optogenetic control of basal ganglia circuitry. Nature, 466(7306), 622–626. https://doi.org/10.1038/nature09159*
31. *Lilascharoen, V., Wang, E. H., Do, N., Pate, S. C., Tran, A. N., Yoon, C. D., Choi, J. H., Wang, X. Y., Pribiag, H., Park, Y. G., Chung, K., & Lim, B. K. (2021). Divergent pallidal pathways underlying distinct Parkinsonian behavioral deficits. Nature neuroscience, 24(4), 504–515. https://doi.org/10.1038/s41593-021-00810-y*
32. *Kaneda, K., & Kita, H. (2005). Synaptically released GABA activates both pre- and postsynaptic GABA(B) receptors in the rat globus pallidus. Journal of neurophysiology, 94(2), 1104–1114. https://doi.org/10.1152/jn.00255.2005*
33. *Kupferschmidt, D. A., & Lovinger, D. M. (2015). Inhibition of presynaptic calcium transients in cortical inputs to the dorsolateral striatum by metabotropic GABA(B) and mGlu2/3 receptors. The Journal of physiology, 593(10), 2295–2310. https://doi.org/10.1113/JP270045*
34. *Kushmerick, C., Price, G. D., Taschenberger, H., Puente, N., Renden, R., Wadiche, J. I., Duvoisin, R. M., Grandes, P., & von Gersdorff, H. (2004). Retroinhibition of presynaptic Ca2+ currents by endocannabinoids released via postsynaptic mGluR activation at a calyx synapse. The Journal of neuroscience : the official journal of the Society for Neuroscience, 24(26), 5955–5965. https://doi.org/10.1523/JNEUROSCI.0768-04.2004*
35. *Brian R. Isett, Katrina P. Nguyen, Jenna C. Schwenk, Christen N. Snyder, Kendra A. Adegbesan, Ugne Ziausyte, Aryn H. Gittis (2022) The Indirect Pathway of the Basal Ganglia Promotes Negative Reinforcement, But Not Motor Suppression, bioRxiv, 2022.05.18.492478; doi: https://doi.org/10.1101/2022.05.18.492478*
36. *Manz, K. M., Baxley, A. G., Zurawski, Z., Hamm, H. E., & Grueter, B. A. (2019). Heterosynaptic GABAB Receptor Function within Feedforward Microcircuits Gates Glutamatergic Transmission in the Nucleus Accumbens Core. The Journal of neuroscience : the official journal of the Society for Neuroscience, 39(47), 9277–9293. https://doi.org/10.1523/JNEUROSCI.1395-19.2019*
37. *Pamukcu, A., Cui, Q., Xenias, H. S., Berceau, B. L., Augustine, E. C., Fan, I., Chalasani, S., Hantman, A. W., Lerner, T. N., Boca, S. M., & Chan, C. S. (2020). Parvalbumin+ and Npas1+ Pallidal Neurons Have Distinct Circuit Topology and Function. The Journal of neuroscience : the official journal of the Society for Neuroscience, 40(41), 7855–7876. https://doi.org/10.1523/JNEUROSCI.0361-20.2020*
38. *Robbe, D., Alonso, G., Duchamp, F., Bockaert, J., & Manzoni, O. J. (2001). Localization and mechanisms of action of cannabinoid receptors at the glutamatergic synapses of the mouse nucleus accumbens. The Journal of neuroscience : the official journal of the Society for Neuroscience, 21(1), 109–116. https://doi.org/10.1523/JNEUROSCI.21-01-00109.2001*
39. *Wallmichrath, I., & Szabo, B. (2002). Cannabinoids inhibit striatonigral GABAergic neurotransmission in the mouse. Neuroscience, 113(3), 671–682. https://doi.org/10.1016/s0306-4522(02)00109-4*
40. *Wu, L. G., & Saggau, P. (1995). GABAB receptor-mediated presynaptic inhibition in guinea-pig hippocampus is caused by reduction of presynaptic Ca2+ influx. The Journal of physiology, 485 (Pt 3)(Pt 3), 649–657. https://doi.org/10.1113/jphysiol.1995.sp020759*
41. *Zurawski, Z., Thompson Gray, A. D., Brady, L. J., Page, B., Church, E., Harris, N. A., Dohn, M. R., Yim, Y. Y., Hyde, K., Mortlock, D. P., Jones, C. K., Winder, D. G., Alford, S., & Hamm, H. E. (2019). Disabling the Gβγ-SNARE interaction disrupts GPCR-mediated presynaptic inhibition, leading to physiological and behavioral phenotypes. Science signaling, 12(569), eaat8595. https://doi.org/10.1126/scisignal.aat8595*